Highly Thermally Conductive Hybrid Carbon Fiber Polymer Composite for Radiator Application

Jin Ho Kang¹ and Keith L. Gordon²

Advanced Materials and Processing Branch, NASA Langley Research Center, Hampton, VA, 23681, USA

Darwyn Ward³

NASA Interns, Fellows, and Scholars (NIFS) Program, NASA Langley Research Center, Hampton, VA 23681, USA

Grace Belancik⁴

Bioengineering Branch, NASA Ames Research Center, Mountain View, CA 94035, USA

Pranav Jagtap⁵

KBR / NASA Ames Research Center, Mountain View, CA 94035, USA

and

Godfrey Sauti⁶

Advanced Materials and Processing Branch, NASA Langley Research Center, Hampton, VA, 23681, USA

Carbon fiber (CF) reinforced polymer composites have been used for aerospace structures because they have low mass, high specific strength, high specific stiffness, and low life-cycle maintenance compared to aluminum alloys. However, due to their relatively low thermal conductivity, pristine CF polymer composites fail to provide effective heat flow for certain applications such as heat exchange systems and radiators. The technology described in this paper provides novel CF polymer composites that possess high thermal conductivity by incorporating pyrolytic graphite sheets (PGS). The thermal conductivities of novel hybrid PGS/CF polymer composites were measured to be about 13 to 36 times higher than that of pristine CF polymer composite, and about two times higher than that of aluminum alloy 6061. This new material with sufficient thermal conductivity is applicable to composite radiators of heat exchange systems.

Nomenclature

 ε_T = Thermal Emissivity α_S = Solar Absorptivity λ = Wavelength CF = Carbon Fiber

CNT = Carbon Nanotube ELC = Express Logistics Carrier

Ep = Epoxy

ISS = International Space Station

¹ Material Research Engineer, Advanced Materials & Processing Branch, NASA Langley Research Center, MS 226.

² Senior Material Research Engineer, Advanced Materials & Processing Branch, NASA Langley Research Center, MS 226.

³ Intern, Advanced Materials & Processing Branch, NASA Langley Research Center, MS 226.

⁴ Air Revitalization Team Lead, Bioengineering Branch, NASA ARC, MS 239-15.

⁵ Mechanical Engineer, KBR / NASA Ames Research Center, MS 239-15.

⁶ Aerospace Research Engineer, Advanced Materials & Processing Branch, NASA Langley Research Center, MS 226.

MISSE = Material International Space Station Experiment

OSR = Optical Solar Reflector PAN = Polyacrylonitrile

PGS = Pyrolytic Graphite Sheet

PW = Plain Weave

SEM = Scanning Electron Microscopy

SSM = Second Surface Mirror

I. Introduction

Carbon fiber reinforced polymer composites have been used for aerospace structures because they have low mass, high specific strength, high specific stiffness, and low life-cycle maintenance compared to aluminum alloys. However, the relatively low thermal conductivities of carbon fiber (CF) polymer composites fail to provide effective heat flow for certain applications such as heat exchanging systems and radiators. The thermal conductivity of carbon fiber polymer composites are about 0.7 W/m·K to 5 W/m·K which is only 0.5% to 3% of that of aluminum alloy 6061. Carbon nanotubes (CNTs) have been known as highly thermally conductive materials. Single-walled CNT has a thermal conductivity of about 200 W/m·K and multiwalled CNT about 3000 W/m·K. Graphene nano-sheets have a similar level of thermal conductivity of CNT. And any research groups have attempted to improve thermal conductivity by incorporating CNTs, graphene nano-sheets or CNT sheets. Pyrolytic graphite sheet (PGS) with a high thermal conductivity of about 400 W/m·K to 1950 W/m·K has been developed and a radiator fabricated with the PGS have been reported. See the strength of the provided the provided that the provided the provided the provided that the provided the provided the provided that the provided that the provided the provided that the provided thas the provided that the provided that the provided that the prov

However, the thermal conductivity for CNTs, graphite nanosheets or CNT sheets incorporated composites was measured to be only about 5 W/m·K to 10 W/m·K which is not high enough for the radiator or heat exchanger applications. Pyrolytic graphite sheets stacked with layers of adhesives have low stiffness and low out-of-plane thermal conductivity due to the adhesive. ¹⁰⁻¹¹ In this study, hybrid CF/PGS epoxy composites were fabricated and the physical properties such as thermal conductivity and thermal optical properties were characterized to replace aluminum alloy which has been used for radiator applications. ¹²⁻¹⁵

II. Experimental

A. Materials

Novolac epoxy (PMT F7*) resin and spread-tow, carbon fiber reinforced epoxy prepreg [Toray M30S polyacrylonitrile (PAN) based carbon fiber plain weave (PW) fabric/epoxy (PMT-F7)] were obtained from Patz Materials and Technology (CA, USA) and used as the baseline composite material. Methyl ethyl ketone (MEK) (Sigma-Aldrich, MO, USA) was used as received to make dilute PMT F7 resin solutions. Several grades of pyrolytic graphitic sheets (PGS) were obtained from two vendors. One set was manufactured by Panasonic Industry (Japan) and the other was manufactured by HPMS Graphite (CA, USA). Pitch based carbon fiber fabrics [Nippon Graphite Fiber (NGF) PF(S)-YSH50A(1k)-75, PF(S)-YSH70A(1k)-75, PF(S)-YS80A(1.5k)-140, SF-YS95A(3k)-200, Japan] were obtained from CST Composite Store (CA, USA). The predetermined amount of PMT F7 solution was painted onto the pitch based NGF carbon fiber fabric to fabricate a "pre-infused" CF/PMT F7 epoxy prepreg sheet with the desired mass fraction (about 50%) of carbon fiber after drying in a convection oven at 60°C for 3 hours, followed by a 50°C in vacuo overnight soak. The dried prepreg and PGS were stacked according to the predetermined layup configuration and cured in an autoclave at 110°C for 1 hour. A pressure of 0.7 MPa was applied and the autoclave was heated at a rate of 3°C/min to 177°C and held for 2 hours, and cooled to ambient temperature. The pressure was then released.

B. Characterization

Thermal conductivity of PGS and hybrid CF/PGS epoxy composites under ambient conditions were measured using a Hot Disk Thermal Constants Analyzer (TPS 2500S, Hot Disk AB, Sweden) with model 5465, 5501, 7280,

^{*}Specific vendor and manufacturer names are explicitly mentioned only to accurately describe the test hardware. The use of vendor and manufacturer names does not imply an endorsement by the U.S. Government nor does it imply that the specified equipment is the best available.

7577 and 102003 sensors. The "slab" mode was employed for measuring in-plane thermal conductivity. Time and heating power for measurement were 1 second to 2 seconds and 25 mW to 300 mW depending on specimen thickness. For out-of-plane conductivity, the "thin film" mode was selected with the measurement time of 10 seconds to 20 seconds and the larger heating power of about 0.8 W to 2 W depending on specimen thickness. Aluminum 6061 T6 was used as a reference material.

The morphology of the sample was studied using a field-emission scanning electron microscope (FE-SEM, S-5200, Hitachi High-Tech, Japan). The accelerating voltage and beam current were 25 KeV to 30 KeV and 17 μ A to 20 μ A, respectively. The specimens were polished as needed using a polisher (Ecomet Polisher, Buehler, IL, USA). The thermo-optical properties [thermal emissivity (ε_T) and solar absorptivity (α_s)] were measured using a portable emissometer (TEMP 2000, AZ Technology, AL, USA) in a wavelength range (λ) of 3 μ m to 30 μ m and a laboratory portable spectroreflectometer (LPSR 300, AZ Technology, Al, USA) in a wavelength range of 250 nm to 2500 nm.

III. Results and Discussion

A. Hybrid CF/PGS Composite Fabrication

PGS is a pyrolytic graphite sheet which consists of highly oriented graphene multilayers. It has high thermal conductivity from 400 W/m·K to 1950 W/m·K, which is up to about five times higher than copper (386 W/m·K) and up to about eight times higher than aluminum (251 W/m·K). The PGS appearance is a dark shade of gray with a partially reflective smooth surface as shown in Figure 1. Four grades of PGS were tested in this study. They were 25 μm and 70 μm thick Panasonic PGS sheets, and 25 μm and 40 μm thick HPMS PGS sheets (Table 1). The SEM images in Figure 2 show the microstructure of PGS 70. Overlays of multiple pieces of thin graphene layer were found in the surface morphology (Figure 2 a-b). The PGS was fractured in liquid nitrogen and the cross-sectional morphology was investigated (Figure 2 c-d) and it was found that the PGS consisted of thin graphene multilayers.

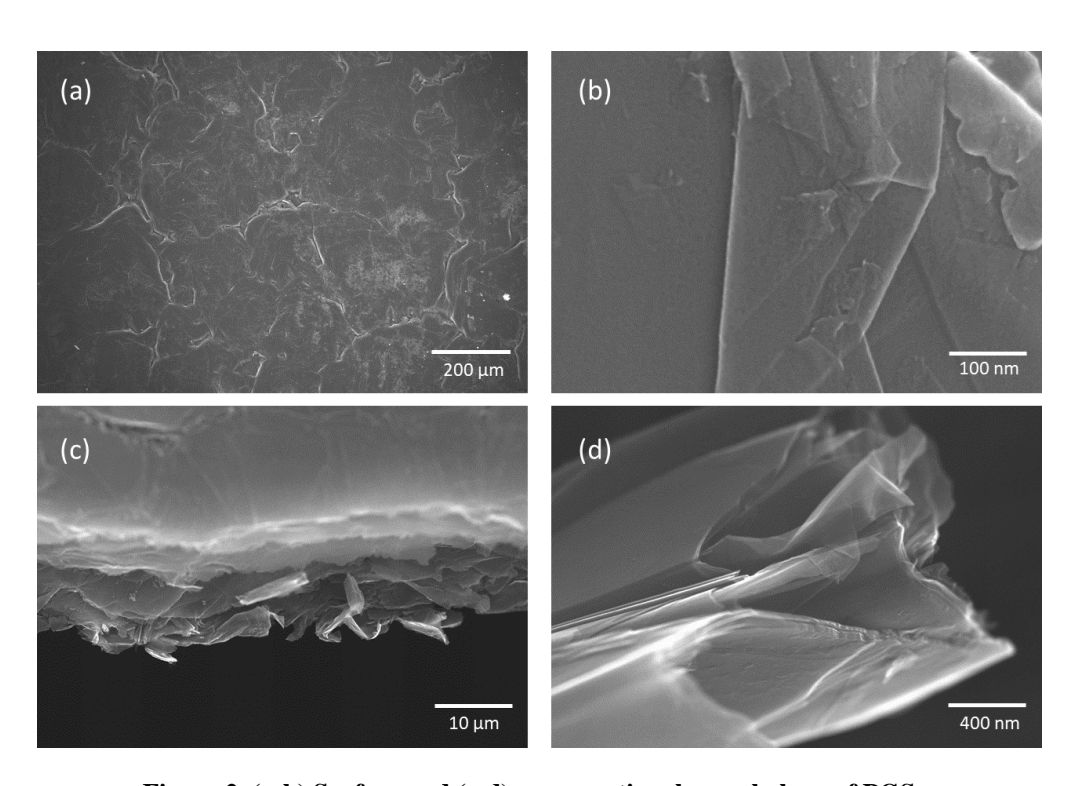


Figure 1. Picture of a PGS.

Table 1. List of samples.

| Sample ID | Specification |
|-------------------------|--|
| Al 6061 | Aluminum 6061 |
| PGS 25 | Panasonic PGS (25 µm thick) |
| PGS 70 | Panasonic PGS (70 µm thick) |
| HPGS 25 | HPMS PGS (25 µm thick) |
| HPGS 40 | HPMS PGS (40 μm thick) |
| CF-Ep | PAN based carbon fiber (M30S) plain weave fabric - Epoxy (PMT F7) composite, 3 plies, $[0-90]_3$ |
| CF-Ep / PGS 25 / CF-Ep | CF-Ep, [0-90], 1 ply / PGS 25, 1ply / CF-Ep, [0-90], 1 ply |
| PGS 25 / CF-Ep / PGS 25 | PGS 25, 1ply / CF-Ep, [0-90], 1 ply / PGS 25, 1ply |

| CF-Ep / PGS 70 / CF-Ep | CF-Ep, [0-90], 1 ply / PGS 70, 1ply / CF-Ep, [0-90], 1 ply |
|---|--|
| PGS 70 / CF-Ep / PGS 70 | PGS 70, 1ply / CF-Ep, [0-90], 1 ply / PGS 70, 1ply |
| PGS 70 / CF / PGS 70 | PGS 70 / CF / PGS 70 |
| CNT_CF-Ep | PAN based carbon fiber (M30S) plain weave fabric - Epoxy (PMT F7) composite doped with 2wt% carbon nanotubes (CNT), [0/90], 1ply |
| p-PGS 70 | Perforated PGS 70 |
| $CNT_CF\text{-}Ep \ / \ p\text{-}PGS \ 70 \ / \ CNT_CF\text{-}Ep$ | CNT_CF-Ep, 1ply / p-PGS 70, 1ply / CNT_CF-Ep, 1ply |
| PCF1-Ep | Pitch based carbon fiber (YS50A) satin weave fabric - Epoxy (PMT F7) composite, 2 plies, $[45]_4$ |
| PCF2-Ep | Pitch based carbon fiber (YS75A) plain weave fabric - Epoxy (PMT F7) composite, 2 plies, $[0-90]_2$ |
| PCF3-Ep | Pitch based carbon fiber (YS80A) plain weave fabric - Epoxy (PMT F7) composite, 2 plies, $[0-90]_2$ |
| PCF4-Ep | Pitch based carbon fiber (YS95A) plain weave fabric - Epoxy (PMT F7) composite, 4 plies, $[0-90]_2$ |
| PCF4-Ep/HPGS 40/PCF4-Ep | PCF4-Ep, [0-90], 1 ply / HPGS 40, 1ply / PCF4-Ep, [0-90], 1 ply |



 $\label{eq:Figure 2. (a-b) Surface and (c-d) cross-sectional morphology of PGS.}$

The hybrid CF/PGS composites were fabricated by laying PGS and CF-epoxy prepreg sheets alternatively. Two layup configurations of the hybrid CF/PGS composites (CF-epoxy/PGS/CF-epoxy composite and PGS/CF-epoxy/PGS composite) are shown in Figure 3 (a,d). All the composites are flexible as shown in Figure 3 (c,f). The sample ID and specification are summarized in Table 1.

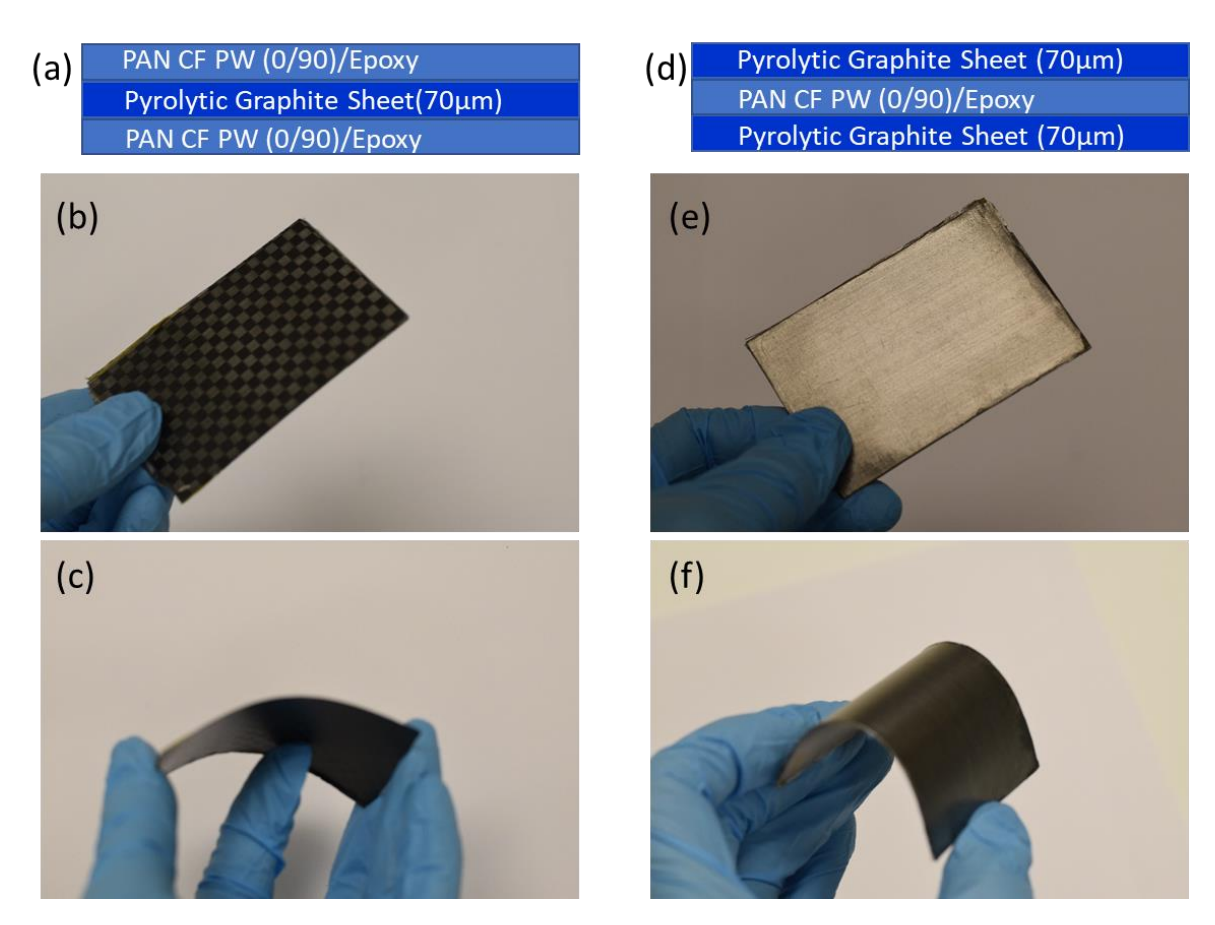


Figure 3. (a) layup configuration and (b-c) fabricated sample of CF-epoxy/PGS 70/CF-epoxy composite, and (d) layup configuration and (e-f) fabricated sample of PGS 70/CF-epoxy/PGS 70 composite.

Cross-sectional micrography was performed to investigate the layered structure of the hybrid CF/PGS epoxy composite. The specimen was fractured in liquid nitrogen and the surface was investigated using SEM. The morphology shown in Figure 4 is the rough fracture surface of CF-epoxy layers for top and bottom and PGS layer in the middle of specimen. However, the interface between the layers could not be clearly identified. Therefore, the fractured sample was polished. The polished cross-section of fracture surface was clearly shown in Figure 5. Good infusion of epoxy resin at the interfaces between CF and PGS as well as clear morphology of CF and PGS were found in the hybrid CF/PGS epoxy composite.

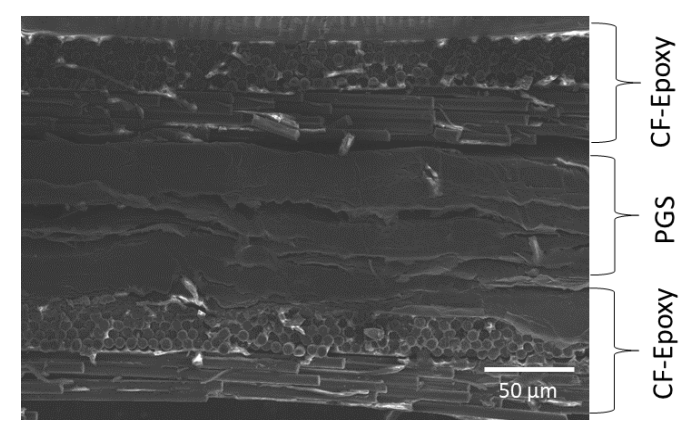


Figure 4. Cross-sectional morphology of CF-epoxy/PGS 70/CF-epoxy composite.

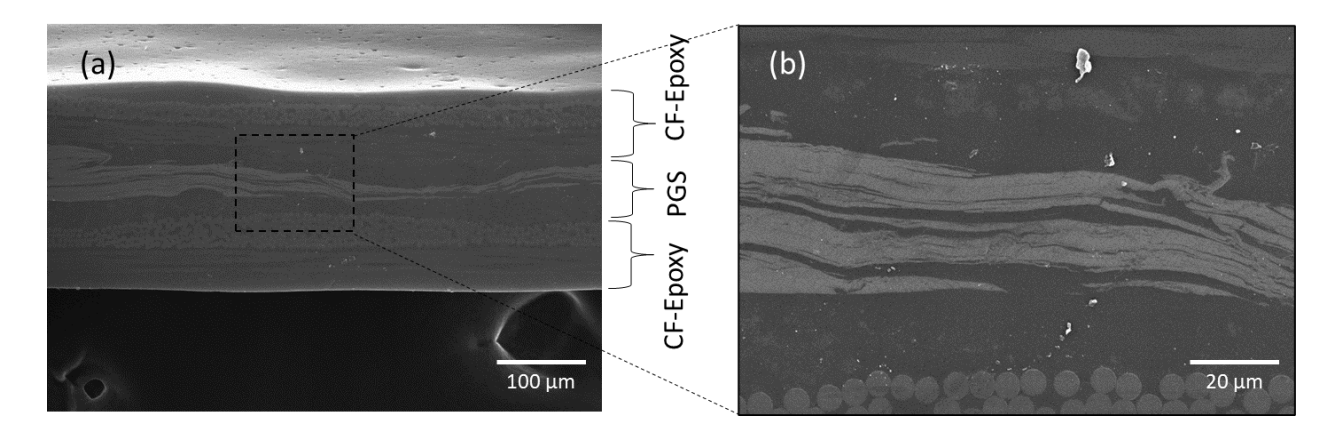


Figure 5. Cross-sectional morphology of CF-epoxy/PGS 70/CF-epoxy composite after polishing.

B. Thermal Conductivity Characterization

The thermal conductivities of the prepared hybrid PGS/CF epoxy composite were measured by the hot disk method. The hot disk technique has been used to study isotropic and anisotropic bulk thermal transport of materials. 16-18 This technique utilizes a "disk" shape sensor which applies the current to make the sensor and material "hot" according to Joule's heating. By monitoring the voltage and current variation over time which are dependent on the material properties, the thermal properties of material were calculated. This technique has the advantages of being able to measure the thermal conductivity, thermal diffusivity, and specific heat capacity of as-prepared materials in solids, liquids, and powders. The in-plane thermal conductivity was measured using the "slab" mode. The in-plane thermal conductivity of PGS 25 and PGS 70 were about 362 W/m·K to 406 W/m·K, and that of HPGS 25 and HPGS 40 were about 501 W/m·K to 544 W/m·K. Thinner PGS has slightly higher thermal conductivity. The baseline CF-Epoxy composite has a thermal conductivity of about 9 W/m·K. When it was

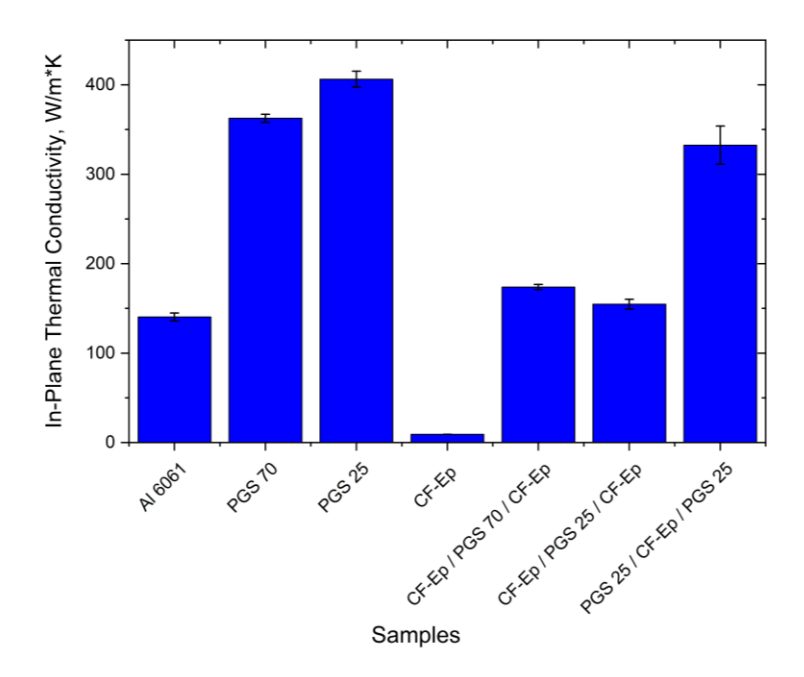


Figure 6. In-plane thermal conductivity of PGS and CF-Epoxy/PGS composite.

laminated with PGS25, the thermal conductivity increased dramatically. The thermal conductivities of CF-Epoxy/PGS 25/CF-Epoxy/PGS 25/CF-Epoxy/PGS 25 were about 155 W/m·K and 333 W/m·K, respectively, as shown in Figure 6. These values are up to about 140% higher than the reference aluminum 6061 (about 140 W/m·K, measured using the isotropic mode) and 3500% higher than the baseline CF-Epoxy composite. The in-plane thermal conductivity of the composite with PGS 70, CF-Epoxy/PGS 70/CF-Epoxy, was about 174 W/m·K, higher than CF-Epoxy/PGS 25/CF-Epoxy composite. The higher thermal conductivity of CF-Epoxy/PGS 70/CF-Epoxy seems to originate from the higher thermal transport through thicker PGS, because the difference in thermal conductivity of PGS 25 and PGS 70 is small. The error bars in the graph represented the standard deviation of the measured values showing the good reliability of experiments.

Table 2. Thermal conductivities of PGS and Hybrid CF/PGS composites.

| Sample | In-Plane Thermal Conductivity (W/m·K) | Out-of-plane Thermal Conductivity (W/m·K) | |
|----------------------------------|--|--|--|
| Al 6061 | 140.48 ± 4.45 | - | |
| PGS 25 | 406.32 ± 8.95 | - | |
| PGS 70 | 362.66 ± 4.44 | - | |
| HPGS 25 | 533.92 ± 16.16 | - | |
| HPGS 40 | 501.12 ± 9.94 | - | |
| CF-Ep | 9.25 ± 0.01 | 0.14 ± 0.02 | |
| CF-Ep / PGS 25 / CF-Ep | 154.75 ± 5.57 | 0.24 ± 0.01 | |
| PGS 25 / CF-Ep / PGS 25 | 332.62 ± 21.33 | 0.04 ± 0.00 | |
| CF-Ep / PGS 70 / CF-Ep | 173.85 ± 2.89 | 0.09 ± 0.02 | |
| CNT_CF-Ep / p-PGS 70 / CNT_CF-Ep | 123.56 ± 0.96 | 0.33 ± 0.01 | |
| PCF1-Ep | 26.55 ± 0.60 | | |
| PCF2-Ep | 42.38 ± 0.50 | | |
| PCF3-Ep | 75.67 ± 0.90 | 0.23 ± 0.00 | |
| PCF4-Ep | 89.48 ± 1.71 | 0.12 ± 0.00 | |
| PCF4-Ep/HPGS 40/PCF4-Ep | 143.1 ± 2.64 | 0.31 ± 0.01 | |

The out-of-plane thermal conductivities of the hybrid composites were measured using the "thin film" mode. The thin film mode was designed for measuring the out-of-plane thermal conductivity of thin film or coating which is thinner than 500 µm by measuring the thermal resistance. The thickness of test samples was about 210 µm to 220 µm. The out-of-plane thermal conductivity of the baseline CF-Epoxy composite was measured to be 0.14 W/m·K (Figure 7 and Table 2). To improve the outof-plane thermal conductivity, carbon nanotubes (CNTs) were infused in the epoxy resin and PGS was perforated for better through-thickness thermal transport by allowing resin and CNTs to flow between layers. The CNTs infusion in CF-epoxy resin and lamination of the perforated PGS improved the out-of-plane thermal conductivity by about 140% ($\Delta \sim 0.19 \text{ W/m·K}$) as shown in Figure 7, but it is still significantly lower than in-plane thermal conductivities. Other concepts of improving out-of-plane e thermal conductivity are under design.

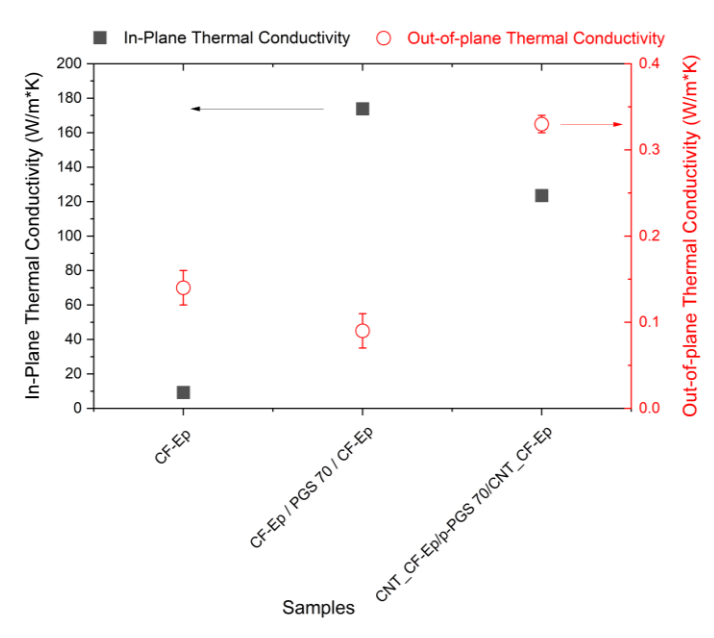


Figure 7. In-plane and out-of-plane thermal conductivity of CF-Epoxy/PGS composite and CNT_CF-Epoxy/perforated PGS composite.

The effect of various carbon fibers on the thermal conductivity of composites investigated using pitch based carbon fiber (Figure 8). Four different grades of pitch based carbon fiber fabrics [PF(S)-YSH50A(1k)-75, PF(S)-YSH70A(1k)-75, PF(S)-YS80A(1.5k)-140 and SF-YS95A(3k)-200] were used to fabricate the hybrid CF/PGS epoxy composites (Table 1). The pitch based CF-epoxy composite was found to have about 190% to 870% higher thermal conductivities (about 27 W/m·K to 89 W/m·K) compared to the PAN based CF-epoxy composite (CF-Ep). Thermal conductivity of higher modulus CF (YS95A, 972 GPa) epoxy composite (PCF4-Ep) was measured to be about 89 W/m·K whereas the thermal conductivity of lower modulus CF (YS50A, 524 GPa) epoxy composite (PCF1-Ep) was measured to be about 27 W/m·K. When PGS (HPGS 40) was laminated with PCF4, the thermal conductivity was about 143 W/m·K.

C. Thermal Optical Properties

Thermal radiation is the main mode of thermal energy transfer via emission of electromagnetic wave in the vacuum of the space, governed by Planck's law and Stefan-Boltzmann's law, and is dependent on the thermal emissivity of materials. Thus, the thermal emissivity of a material is important to estimate the total emissive power from the radiator. The thermal emissivity of PGS ranges from about 0.32 to 0.34 as shown in Figure 9 and Table 3. The thermal emissivities of CFepoxy laminated PGS, CF-Epoxy/PGS 25 (or PGS 70)/CF-Epoxy were measured to be about 0.74 to 0.76. The thermal emissivity of PGS laminated on CF-Epoxy layer was about 0.30, which is similar to that of PGS itself, because PGS is exposed to free space. The infusion of CNT into epoxy resin increased the thermal emissivity to about 0.89, which is similar to the commercial coating, Aeroglaze Z307 ($\varepsilon_T \sim 0.89$). This means CNT infused CF-Epoxy Composite radiator may eliminate the need for additional black thermal coating.

When an object is exposed to sun light, the solar absorptivity of material is another key parameter to determine the thermal equilibrium in space. Therefore, the solar absorptivity was

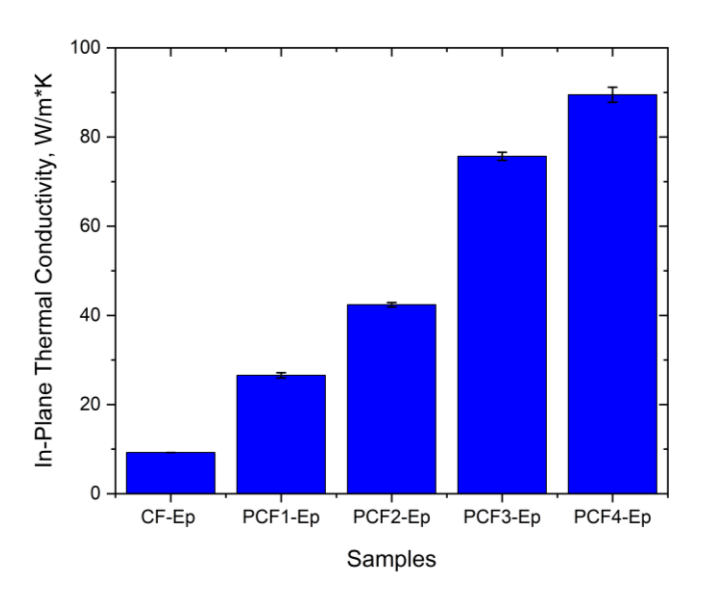


Figure 8. In-plane thermal conductivity of pitch based CF-Epoxy/PGS composite.

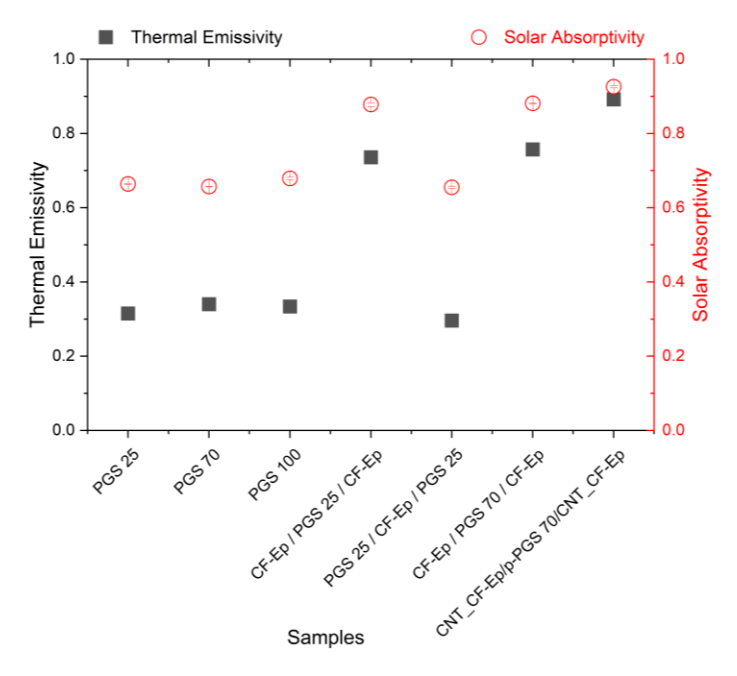


Figure 9. Thermal emissivity (ε_T) and solar absorptivity (α_s) of PGS and CF-Epoxy/PGS composite.

measured using a spectroreflectometer. The solar absorptivity of samples was higher than the thermal emissivity as shown in Figure 9 and Table 3. The solar absorptivity of PGS and PGS laminated CF-Epoxy composite (PGS 25/CF-Ep/PGS 25) ranges from about 0.66 to 0.68. The solar absorptivity of CF-epoxy laminated PGS composites [CF-Epoxy/PGS 25 (or PGS 70)/CF-Epoxy] and CNT infused CF-Epoxy composite was measured to be about 0.88 to 0.93. The ratio $\alpha_{\rm c}$, $\ell_{\rm c}$ is higher than 1.0. This result indicated that white thermal coating, optical solar reflector (OSR)

or second surface mirror (SSM) which has low α_s and high ϵ_T will be required for the Sun-facing surface of the composite radiator.

The environmental effect on thermal optical properties has been under evaluation with Material International Space Station Experiment (MISSE) 17 flight test. Samples were installed at Express Logistics Carrier (ELC) 2 of the International Space Station (ISS) on March 28, 2023 to April 3, 2023, and has been exposed to space environment for the zenith direction since April 5, 2023. After about 6 month flight, the samples will be retrieved to evaluate the material properties including thermal optical properties and thermal conductivities.

Table 3. Thermal emissivity and solar absorptivity of PGS and CF/PGS composites.

| Sample | Thermal Emissivity (ε_T , λ : 3 μ m to 30 μ m) | Solar Absorptivity (α_S , λ : 250 nm to 2500 nm) | $\alpha_{_{S}}$, / ε_{T} |
|-------------------------------|---|--|---------------------------------------|
| PGS 25 | 0.315 ± 0.001 | 0.664 ± 0.001 | 2.108 |
| PGS 70 | 0.340 ± 0.000 | 0.657 ± 0.001 | 1.932 |
| PGS 100 | 0.334 ± 0.001 | 0.679 ± 0.003 | 2.033 |
| CF-Ep / PGS 25 / CF-Ep | 0.736 ± 0.000 | 0.878 ± 0.005 | 1.193 |
| PGS 25 / CF-Ep / PGS 25 | 0.296 ± 0.001 | 0.665 ± 0.003 | 2.247 |
| CF-Ep / PGS 70 / CF-EP | 0.757 ± 0.000 | 0.881 ± 0.001 | 1.164 |
| CNT_CF / p-PGS 70 / CNT_CF-Ep | 0.892 ± 0.001 | 0.926 ± 0.003 | 1.038 |

IV. Conclusion

Highly thermally conductive composites for potential radiator and heat exchanger applications were fabricated with various carbon fiber (CF) fabrics and pyrolytic graphite sheets (PGS). The pitch based CF-epoxy composites were found to have about an 870% improvement in thermal conductivity compared to PAN based-CF-epoxy composites. The in-plane thermal conductivity of the PGS laminated CF-epoxy composites was about 333 W/m·K, 3500% higher than the baseline CF-Epoxy composite and about 140% higher than the reference aluminum 6061. Thermal emissivity of the CF-Epoxy/PGS composites varied from about 0.32 to 0.76 based on the exposed material. The addition of CNT in CF-Epoxy resin increased the thermal emissivity to about 0.89 and might eliminate the use of black thermal coating (high ε_T) for the back side of a radiator. However, the solar absorptivity of composite were about 0.67 to 0.93 and the ratio α_S , ℓ_T is higher than 1.0. Therefore, white thermal coating, OSR or SSM (low α_S and high ε_T) will be required for the Sun-facing surface of the radiator. The new material possesses sufficient thermal conductivity in the in-plane direction, but needs further study to improve its out-of-plane thermal conductivity. In addition, other material parameters such as density, specific strength, and thermal expansion coefficient will be evaluated for composite radiator panel applications, and the design of a composite radiator and thermal transport analysis will be performed with the next work.

Acknowledgements

The authors would like to thank the Exploration Capabilities program, Life Support Systems project for financially supporting their efforts described in this publication, and Mr. Zane Green for sample preparation and analysis.

References

- ¹Kang, J. H., Cano, R. J., Ratcliffe, J. G., Luong, H., Grimsley, B. W., and Siochi, E. J., "Multifunctional Hybrid Carbon Nanotube/Carbon Fiber Polymer Composites," *SAMPE 2016*, Society for the Advancement of Material and Process Engineering, Long Beach, CA, 2016, pp. 15.
- ²Hone, J., Liaguno, M. C., Nemes, N. M., Johnson, A. T., Fischer, J. E., Walters, D. A., Casavant, M. J., Schmidt, J., and Smalley, R. E., "Electrical and Thermal Transport Properties of Magnetically Aligned Single Wall Carbon Nanotube Film," *Applied Physical Letters*, Vol. 77, Iss. 5, 2000, pp. 666-668.
- ³Kim, P., Shi, L., Majumdar, A., and McEuen, P. L., "Thermal Transport Measurements of Individual Multiwalled Nanotubes," *Physical Review Letters*, Vol. 87, 2001, pp. 215502.
- ⁴Ghose, S., Working, D. C., Connell, J. W., Smith, J. G., Watson, K. A., Delozier, D. M., Sun, Y. P, and Lin, Y., "Thermal Conductivity of UltemTM/Carbon Nanofiller Blends," *High Performance Polymers*, Vol., 18, Iss. 6, 2006, pp. 961-977.
- ⁵Kalaitzidou, K., Fukushima, H., and Drzal, L. T., "Multifunctional Polypropylene Composites Produced by Incorporation of Exfoliated Graphite Nanoplatelets," *Carbon*, Vol. 45, 2007, pp. 1446-1452.
- ⁶Inagaki, M., Kaburagi, Y., and Hishiyama, Y., "Thermal Management Material: Graphite," *Advanced Engineering Materials*, Vol. 16, No. 5., pp. 494-506.
- ⁷Murakami, M., Watanabe, K., and Yoshimura, S., "High-Quality Pyrographite Films," *Applied Physics Letters*, Vol. 48, 1986, pp. 1594.
- ⁸Nagano, H., Ohnishi, A., and Nagasaka, Y., "Thermophysical Properties of High-Thermal-Conductivity Graphite Sheets for Spacecraft Thermal Design," *Journal of Thermophysics and Heat Transfer*, Vol. 15, No. 3, 2001, pp. 347-353.
- ⁹Mena, F., and Benthem, B., Airbus Defense and Space SAS, Toulouse, France, US Patent for "Flexible Radiative Fin for a Spacecraft," Patent No. 11,254,452, issued 21 June 2019.
- ¹⁰Mass, A., "Development of Pyrolytic Graphite Applications in Spacecraft Thermal Control Systems," 47th International Conference on Environmental System Proceedings, ICES, Charleston, SC, July 2017.
- ¹¹De Groot, T., Schwieters, B., Van Benthem, R., Van Es, Johannes, and Pauw, A., "Breadbod Testing of a HiPeR Inflatable Radiator (HiPeR INFRA)," 49th International Conference on Environmental Systems, ICES, Boston, MA, 2019.
- ¹²Belancik, G., Jan, D., and Huang, R., "Spacecraft Carbon Dioxide Deposition Subscale System Design and Test," *International Conference on Environmental Systems Proceedings*, ICES, Boston, MA, July 2019.
- ¹³Belancik, G., Schuh, M., Jan, D., and Jagtap, P., "Evaluation Capabilities of the Carbon Dioxide Deposition System," 50th International Conference on Environmental Systems Proceedings, ICES, online, July 2020.
- ¹⁴Jagtap, P., Belancik, G., Jan, D., Chen, W., and Hall, S., "Power Optimization of Cryogenic CO₂ Deposition Capture in Deep Space," 50th International Conference on Environmental Systems Proceedings, ICES, online, July 2020.
 ¹⁵Jagtap, P., Costa, T., Belancik, G., Schuh, M., Samson, J., Gan, K., "Spacecraft Carbon Dioxide Deposition Full-Scale System:
- ¹⁵Jagtap, P., Costa, T., Belancik, G., Schuh, M., Samson, J., Gan, K., "Spacecraft Carbon Dioxide Deposition Full-Scale System: Design, Analysis, Build and Test," *52nd International Conference on Environmental Systems Proceedings*, ICES, Calgary, Canada, July 2023 (to be published).
- ¹⁶Gustafsson, S. E., "Transient Plane Source Techniques for Thermal Conductivity and Thermal Diffusivity Measurements of Solid Materials," *Review of Scientific Instruments*, Vol. 62, No. 3, 1991, pp. 797-804.
- ¹⁷Log, T., and Gustafsson, S. E., "Transient Plane Source (TPS) Technique for Measuring Thermal Transport Properties of Building Materials," *Fire and Materials*, Vol. 19, No. 1, 1995, pp. 43-49.
- ¹⁸Gustavsson, M., and Hälldahl, L., "Thermal Conductivity Measurement of Thin Insulating Layers Deposited on High-Conducting Sheets," *International Journal of Thermophysics*, Vol. 27, No. 1, 2006, pp. 195-207.